Available online at www.sciencedirect.com
ScienceDirect
Thin-Walled Structures 46 (2008) 112–121
THIN-WALLED STRUCTURES
www.elsevier.com/locate/tws

Vibrations of axially moving flexible beams made of functionally graded materials

M.T. Piovan[a,*], R. Sampaio[b]

[a]Mechanical Systems Analysis Group, Universidad Tecnológica Nacional - Facultad Regional Bahía Blanca, 11 de Abril 461, B8000LMI Bahía Blanca, BA, Argentina
[b]Department of Mechanical Engineering, Pontifícia Universidade Católica - Rio de Janeiro. Rua Marquês de São Vicente 225, 22453-900 Rio de Janeiro, RJ, Brazil

Received 4 July 2007; received in revised form 15 August 2007; accepted 16 August 2007
Available online 24 October 2007

Abstract

Problems related to the vibrations of axially moving flexible beams made of functionally graded materials are addressed. The problem of an axially moving beam may be interpreted as a telescopic system in which the mass is not constant, the mechanism of elastic deformation is transverse bending. A thin-walled beam with annular cross-section is analyzed, in which a continuously graded variation in the composition of ceramic and metal phases across the wall thickness with a simple power law is considered. In this paper a finite element scheme is employed to obtain numerical approximations to the variational equation of the problem. Normally, finite element approaches use fixed-size elements, however, for this kind of problems the increase of the number of elements, step by step as the mass enters, is a cumbersome task. For this reason an approach based on a beam-element of variable domain is adopted. The length of the element is a prescribed function of time. Results highlighting the effects of the beam flexibility, tip mass and material constituents on the dynamics of the axially moving beams are presented and the corresponding conclusions are given.

Keywords: Axially moving beams; Functionally graded materials; Non-conventional finite elements

1. Introduction

Axially moving beams appear in a broad range of problems such as telescopic robotic manipulators, deployment of flexible antennas or appendages of spacecrafts, band-saw blades, as well as the rolling process of plates, wire rods, recorder tapes and belts, among others. In this kind of problems the conservation of mass is not automatically satisfied because mass may change depending on the type of boundary conditions. That is, if the axially moving beam is considered to be inextensible or axially rigid and it is supported between two fixed points (the case of belts or band-saw blades), the mass of the system in the domain can be conserved if the motion amplitude is small. However, in the case of telescopic cantilevered beam (the case of robot arms), the mass of the system is not conserved as mass enters or leaves the domain. In this class of problems, the rate of entering mass is a prescribed value. The study of flexible beams in a translational axial movement have been gaining attention in the last years [1–7] due to new applications in the areas of robotics and spacecrafts, specifically modeling telescopic flexible actuators traveling through prismatic joints. These last applications may operate under severe environmental conditions, such as high temperatures, requiring an extended operational life. Under these circumstances, the use of functionally graded materials can offer some constructive answers in order to avoid possible structural limitations.

The functionally graded materials are a kind of composite whose properties vary continuously and smoothly from a ceramic surface to a metallic surface in a specified direction of the structure. The ceramic face protects the metallic surface from corrosion as well as thermal failure, whereas the metallic part offers strength and stiffness to the

*Corresponding author. Tel.: +54 291 4555 220; fax: +54 291 4555 311.
E-mail address: mpiovan@frbb.utn.edu.ar (M.T. Piovan).

0263-8231/$ - see front matter © 2007 Elsevier Ltd. All rights reserved.
doi:10.1016/j.tws.2007.08.031

structure. The material properties are normally modeled varying according to a power law along the thickness of a shell [8] that constitutes the structure. The research in structural problems, focusing attention in the employment of functionally graded materials, has been mainly devoted to eigenvalue analysis of beams [9], plates and shells [8]. However, to the best of the authors's knowledge, in spite of its importance, no research work related to the vibrations of axially moving flexible beams made of functionally graded materials has been yet presented.

In the present work, a study on the vibrations of flexible sliding beams made of functionally graded materials, deployed or retrieved through a prismatic joint, is performed. The beam is modeled employing Euler–Bernoulli assumptions for small displacements and deformations [1,4]. A finite element scheme is employed to obtain numerical approximations to the variational equation of the problem. Normally, finite element approaches use fixed-size elements, however, for this kind of problems the increase of the number of elements, step by step as the mass enters, is a cumbersome task that needs a very large number of small elements in order to reach reasonable smoothness and accuracy in the results. Al-Bedoor and Khulief [6,7] developed a finite element scheme where a transition element is employed in the link as the mass enters. Although the use of transition element is an interesting idea, it presents some inconveniences in the programming stage because one has to consider that the element is partially housed in the hub, then without flexural deformation. For this reason an approach based on a beam-element of variable domain [1] is adopted in this work, where the length of the element is a prescribed function of the time. The finite element methodology is revisited in order to make clear its use in the context of a beam constructed with functionally graded materials. A study of dynamic responses for different cases of axial deploying patterns and material configurations is performed.

2. Structural model

2.1. Basic assumptions

Fig. 1 shows a horizontal flexible beam of variable length $L(t)$ moving along its longitudinal x-axis at a prescribed velocity, $V = \partial_t L(t)$. The beam has a total length L_T, and an annular cross-section, where the material properties are functionally graded in the thickness. The following hypotheses are considered in order to develop the model: (a) Bernoulli–Euler assumptions are invoked to model the structure, i.e., the cross-section is preserved from distortions in its plane, rotary inertia effects and the extensional deformation are neglected, i.e. only transverse bending is considered; (b) the gravitational potential energy due to the elastic deformations is not taken into account in comparison to the overall reference motion; (c) a tip mass is considered to be concentrated at the free end of the beam; (d) The beam is composed by ceramic and metallic phases, where a simple power-law-type definition is employed for the volume fraction of metal (ceramic) in the thickness.

The functionally graded shells are considered to be composed by many isotropic homogeneous layers [10]. The stress–strain relations for a generally isotropic material including thermal effects are expressed as [11]

$$\begin{Bmatrix} \sigma_{xx} \\ \sigma_{ss} \\ \sigma_{xn} \\ \sigma_{ns} \\ \sigma_{xs} \end{Bmatrix} = \begin{bmatrix} Q_{11} & Q_{12} & 0 & 0 & 0 \\ Q_{12} & Q_{11} & 0 & 0 & 0 \\ 0 & 0 & Q_{44} & 0 & 0 \\ 0 & 0 & 0 & Q_{55} & 0 \\ 0 & 0 & 0 & 0 & Q_{66} \end{bmatrix} \times \left(\begin{Bmatrix} \varepsilon_{xx} \\ \varepsilon_{ss} \\ \varepsilon_{xn} \\ \varepsilon_{ns} \\ \varepsilon_{xs} \end{Bmatrix} - \begin{Bmatrix} \hat{\alpha}\Delta T \\ \hat{\alpha}\Delta T \\ 0 \\ 0 \\ 0 \end{Bmatrix} \right). \tag{1}$$

The matrix elements Q_{ij} are defined in terms of effective elastic properties:

$$Q_{11} = \frac{E_{eff}}{1-\nu_{eff}^2}, \quad Q_{12} = \frac{E_{eff}\nu_{eff}}{1-\nu_{eff}^2}, \quad Q_{44} = Q_{55} = Q_{66} = \frac{E_{eff}}{2(1+\nu_{eff})}, \quad \hat{\alpha} = \frac{\alpha_{eff}}{1-\nu_{eff}}. \tag{2}$$

As the Euler–Bernoulli hypotheses are invoked, only the first two components of stress and strain of Eq. (1) would be employed.

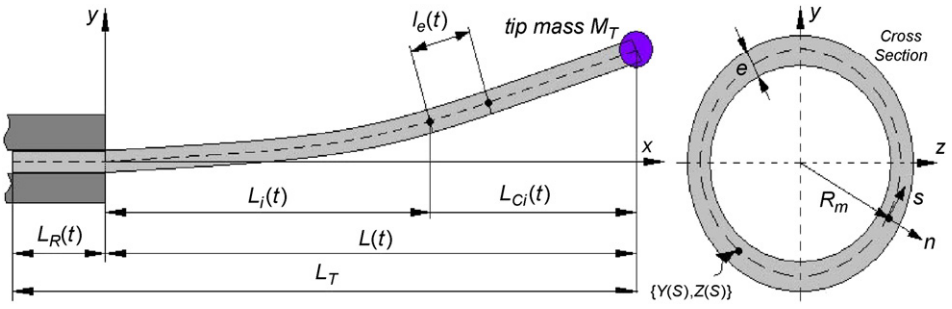

Fig. 1. Beam configuration

The material properties are given by

$$E_{eff}(n) = (E_o - E_i)\left(\frac{2n+e}{2e}\right)^K + E_i, \tag{3}$$

$$v_{eff}(n) = (v_o - v_i)\left(\frac{2n+e}{2e}\right)^K + v_i, \tag{4}$$

$$\alpha_{eff}(n) = (\alpha_o - \alpha_i)\left(\frac{2n+e}{2e}\right)^K + \alpha_i, \tag{5}$$

$$\rho_{eff}(n) = (\rho_o - \rho_i)\left(\frac{2n+e}{2e}\right)^K + \rho_i, \tag{6}$$

$$\kappa_{eff}(n) = (\kappa_o - \kappa_i)\left(\frac{2n+e}{2e}\right)^K + \kappa_i \tag{7}$$

in which E_{eff}, v_{eff}, α_{eff} and ρ_{eff} are the effective modulus of elasticity, effective Poisson's coefficient, effective thermal expansion coefficient and effective mass density, respectively. These properties are defined for $n \in [-e/2, e/2]$, where e is the thickness. The subindexes "o" and "i" stand for outer and inner surfaces, respectively. K ($0 \leqslant K \leqslant \infty$) is the power law exponent. It becomes evident that if $K = 0$ the beam is entirely made of the outer material, normally ceramic. In addition to the exponential laws of variation in the radial direction, the properties may be subjected to variation with the temperature that can be represented by the following expression [8,9]:

$$m_p = m_{p0}(c_0 T^{-1} + 1 + c_1 T + c_2 T^2 + c_3 T^3) \tag{8}$$

in which m_p is a material property in general (i.e., modulus of elasticity, or Poisson's coefficient, etc.), T is the absolute temperature [K] and the coefficients c_i and m_{p0} are unique for a particular material and obtained by means of a curve fitting procedure [12]. Thus the material properties can be represented as a function of the thickness and the temperature. It is assumed, only for simulation and qualitative analysis purposes, that the beam is subjected to a uniform temperature in the whole domain.

2.2. Variational formulation of the structural member

The displacement field taking into account the hypotheses of the previous paragraph is

$$u_x(x,s,n,t) = -\left[Y(s) - n\frac{\mathrm{d}Z}{\mathrm{d}s}\right]\frac{\partial v(x,t)}{\partial x},$$

$$u_y(x,s,n,t) = v(x,t). \tag{9}$$

The displacement field (9) is a particular case of displacement fields of thin-walled beam formulations (see Refs. [9,13]), in which the points $\{Y(s), Z(s)\}$ describe the middle line of the wall thickness as shown in Fig. 1. Under the hypotheses proposed above, only the axial strain is considered, which can be expressed as

$$\varepsilon_{xx} = \bar{\varepsilon}_{xx} + n\bar{\kappa}_{xx} \tag{10}$$

in which $\bar{\varepsilon}_{xx}$ and $\bar{\kappa}_{xx}$ are given by

$$\bar{\varepsilon}_{xx} = -Y(s)\frac{\partial^2 v}{\partial x^2}, \quad \bar{\kappa}_{xx} = \frac{\mathrm{d}Z}{\mathrm{d}s}\frac{\partial^2 v}{\partial x^2}. \tag{11}$$

Then, the strain energy of this structural member can be described as

$$E_d = \frac{1}{2}\int_0^{L(t)} J_{11}^{11}\left(\frac{\partial^2 v}{\partial x^2}\right)^2 \mathrm{d}x. \tag{12}$$

The kinetic energy of the system may be expressed as

$$E_k = \frac{1}{2}\int_0^{L(t)} J_{11}^{\rho}\left[\left(\frac{\partial v}{\partial t} + \frac{\partial x(t)}{\partial t}\frac{\partial v}{\partial x}\right)^2 + \underline{\frac{\partial V}{\partial t}(L(t) - x(t))\left(\frac{\partial v}{\partial x}\right)^2}\right]\mathrm{d}x + \underline{\underline{\frac{1}{2}J_{11}^{\rho}L_T V^2}} + \underline{\underline{\frac{1}{2}M_T\left(\frac{\partial v(L(t),t)}{\partial t}\right)^2}}. \tag{13}$$

In expressions (12) and (13), $L(t)$ is the instantaneous length of the protruded part of the sliding beam. In expression (13), the first term, the underlined term and the double underlined term correspond to the transverse complementary kinetic energy, the kinetic energy due to axial acceleration (also called co-kinetic energy in Refs. [2,3]) and the complementary longitudinal kinetic energy (or kinetic energy due to the axial motion of the rigid body), respectively. This last term is a prescribed quantity since the sliding velocity $V(t)$ is prescribed. The triple underlined terms corresponds to the kinetic energy of the tip mass M_T. It has to be noted that expressions (12) and (13) are similar to those developed, for the case of isotropic materials, by Stylianou and Tabarrok [1]. Note also that in Eq. (13), $\partial x(t)/\partial t = \partial L(t)/\partial t = V$, due to the condition of inextensibility. The constants J_{11}^{11} and J_{11}^{ρ} are the flexural stiffness and sectional inertia for a functionally graded material, that are given by the following expressions:

$$J_{11}^{11} = \int_0^{2\pi R_m}\left[\bar{A}_{11}Y^2(s) - 2\bar{B}_{11}Y(s)\frac{\mathrm{d}Z}{\mathrm{d}s} + \bar{D}_{11}\left(\frac{\mathrm{d}Z}{\mathrm{d}s}\right)^2\right]\mathrm{d}s, \tag{14}$$

$$J_{11}^{\rho} = \int_0^{2\pi R_m}\int_{-e/2}^{e/2}\rho_{eff}\,\mathrm{d}n\,\mathrm{d}s. \tag{15}$$

In the above expressions ρ_{eff} is obtained from (6); $\bar{A}_{11}$, $\bar{B}_{11}$ and $\bar{D}_{11}$ are modified shell-stiffnesses for functionally graded materials which are obtained eliminating N_{ss} and M_{ss} which are considered negligible as a common procedure for composites materials [13], and reducing $\bar{\varepsilon}_{ss}$ and $\bar{\kappa}_{ss}$ from the following expression:

$$\begin{Bmatrix} N_{xx} \\ N_{ss} \\ M_{xx} \\ M_{ss} \end{Bmatrix} = \begin{bmatrix} A_{11} & A_{12} & B_{11} & B_{12} \\ A_{12} & A_{11} & B_{12} & B_{11} \\ B_{11} & B_{12} & D_{11} & D_{12} \\ B_{12} & B_{11} & D_{12} & D_{11} \end{bmatrix} \begin{Bmatrix} \bar{\varepsilon}_{xx} \\ \bar{\varepsilon}_{ss} \\ \bar{\kappa}_{xx} \\ \bar{\kappa}_{ss} \end{Bmatrix}, \tag{16}$$

where N_{xx} and N_{ss} are shell forces, M_{xx} and M_{ss} are shell moments, and A_{ij}, B_{ij} and D_{ij} are given by

$$\{A_{ij}, B_{ji}, D_{ij}\} = \int_{-e/2}^{e/2} Q_{ij}\{1, n, n^2\}\,\mathrm{d}n. \tag{17}$$

Since this problem has mass entering (or leaving) the system, normally it is described by means of an Eulerian formulation. However, it was shown [2,3] that the Lagrangian formulation can still be used even for the case of a system with changing mass [14]. In these circumstances, the equation of motion can be obtained by the following Lagrangian expression:

$$\delta\mathscr{L} = \delta E_k - \delta E_d = 0. \tag{18}$$

2.3. Finite element discretization

As it was mentioned previously a finite element scheme will be employed to solve the motion equation. The approximation scheme for this sliding beam model for functionally graded materials is based on the concept of variable domain element introduced, for the case of isotropic materials, by Stylianou and Tabarrok [1]. In this context, the length of the element is not considered fixed, but varying accordingly to the prescribed sliding velocity V. In order to develop the finite element equation for the variable domain element, the free part of the sliding beam is divided into a number of equal length elements. Under this circumstances, the Lagrangian (18) for a ith element is given by

$$\delta\mathscr{L}_i = \frac{\delta}{2}\int_0^{l_e(t)} \left\{ J_{11}^{\rho}\left[\frac{\partial\bar{v}}{\partial t} + \frac{\partial L_{Ci}}{\partial t}\frac{\partial\bar{v}}{\partial\bar{x}} + \frac{\partial V}{\partial t}(L_{Ci}-\bar{x})\left(\frac{\partial\bar{v}}{\partial\bar{x}}\right)^2\right] - J_{11}^{11}\left(\frac{\partial^2\bar{v}}{\partial\bar{x}^2}\right)^2 \right\}\mathrm{d}\bar{x} = 0, \tag{19}$$

where the overbar in the variables corresponds to the homonym variables but in the element domain. The location of the spatial variable $\bar{x}(t)$ in the element domain, is given by the following expression:

$$\bar{x}(t) = x(t) - L_i(t). \tag{20}$$

Then, since $\partial x(t)/\partial t = \partial L(t)/\partial t = V$, the velocity of position change in the element domain is given by

$$\frac{\partial\bar{x}(t)}{\partial t} = \frac{\partial x(t)}{\partial t} - \frac{\partial L_i(t)}{\partial t} = \frac{\partial L(t)}{\partial t} - \frac{\partial L_i(t)}{\partial t} = \frac{\partial L_{Ci}(t)}{\partial t}, \tag{21}$$

where, being N_e the number of elements, the complementary length $L_{Ci}(t)$ is given by

$$L_{Ci}(t) = L(t) - L_i(t) = L(t)\left[1 - \frac{i-1}{N_e}\right]. \tag{22}$$

The flexural displacement can be represented by the following vector expression:

$$v = \mathbf{F}^{\mathrm{T}}\mathbf{q}_e \tag{23}$$

in which the shape functions and nodal variables are given by

$$\mathbf{F} = \left\{1 - \frac{3\bar{x}^2}{l_e^2} + \frac{2\bar{x}^3}{l_e^3}, \bar{x} - \frac{2\bar{x}^2}{l_e} + \frac{\bar{x}^3}{l_e^2}, \frac{3\bar{x}^2}{l_e^2} - \frac{2\bar{x}^3}{l_e^3}, -\frac{\bar{x}^2}{l_e} + \frac{\bar{x}^3}{l_e^2}\right\},$$

$$\mathbf{q}_e = \left\{v_1, \frac{\partial v_1}{\partial\bar{x}}, v_2, \frac{\partial v_2}{\partial\bar{x}}\right\}^{\mathrm{T}}. \tag{24}$$

It has to be mentioned that l_e is time dependent consequently the finite element expressions for the derivatives of variable v are

$$\frac{\partial v}{\partial\bar{x}} = \frac{\partial\mathbf{F}^{\mathrm{T}}}{\partial\bar{x}}\,\mathbf{q}_e, \quad \frac{\partial^2 v}{\partial\bar{x}^2} = \frac{\partial^2\mathbf{F}^{\mathrm{T}}}{\partial\bar{x}^2}\,\mathbf{q}_e, \quad \frac{\partial v}{\partial t} = \frac{\partial\mathbf{F}^{\mathrm{T}}}{\partial t}\,\mathbf{q}_e + \mathbf{F}^{\mathrm{T}}\frac{\partial\mathbf{q}_e}{\partial t}. \tag{25}$$

Now, substituting (25) into expression (19), performing variational calculus, integrating in the time variables and arranging in terms of the vector of nodal variables, nodal velocities and nodal accelerations, one can arrive to the following element equation:

$$\mathbf{m}_e\frac{\partial^2\mathbf{q}_e}{\partial t^2} + \mathbf{c}_{eq}\frac{\partial\mathbf{q}_e}{\partial t} + \mathbf{k}_{eq}\mathbf{q}_e = 0, \tag{26}$$

where $\mathbf{m}_e$, $\mathbf{c}_{eq}$ and $\mathbf{k}_{eq}$ are the elementary matrices of mass, equivalent damping and equivalent stiffness, respectively. The elementary mass matrix is given by

$$\mathbf{m}_e = \int_0^{l_e(t)} J_{11}^{\rho}\mathbf{F}^{\mathrm{T}}\mathbf{F}\,\mathrm{d}\bar{x}, \tag{27}$$

whereas the elementary equivalent damping and equivalent stiffness matrices are given by

$$\mathbf{c}_{eq} = \mathbf{c}_{e1} - \mathbf{c}_{e2} + \frac{\partial\mathbf{m}_e}{\partial t},$$

$$\mathbf{k}_{eq} = \mathbf{k}_{e0} - \mathbf{m}_{e1} - \mathbf{m}_{e2} + \frac{\partial\mathbf{c}_{e1}}{\partial t} \tag{28}$$

in which

$$\mathbf{k}_{e0} = \int_0^{l_e(t)} J_{11}^{11}\frac{\partial^2\mathbf{F}^{\mathrm{T}}}{\partial\bar{x}^2}\,\frac{\partial^2\mathbf{F}}{\partial\bar{x}^2}\,\mathrm{d}\bar{x},$$

$$\mathbf{c}_{e1} = \int_0^{l_e(t)} J_{11}^{\rho}\left(\mathbf{F}^{\mathrm{T}}\frac{\partial\mathbf{F}}{\partial t} + \frac{\partial L_{Ci}}{\partial t}\mathbf{F}^{\mathrm{T}}\frac{\partial\mathbf{F}}{\partial\bar{x}}\right)\mathrm{d}\bar{x},$$

$$\mathbf{c}_{e2} = \int_0^{l_e(t)} J_{11}^{\rho}\left(\frac{\partial\mathbf{F}^{\mathrm{T}}}{\partial t}\,\mathbf{F} + \frac{\partial L_{Ci}}{\partial t}\frac{\partial\mathbf{F}^{\mathrm{T}}}{\partial\bar{x}}\,\mathbf{F}\right)\mathrm{d}\bar{x},$$

$$\mathbf{m}_{e1} = \int_0^{l_e(t)} J_{11}^{\rho}\left[\frac{\partial\mathbf{F}^{\mathrm{T}}}{\partial t}\,\frac{\partial\mathbf{F}}{\partial t} + \frac{\partial L_{Ci}}{\partial t}\left(\frac{\partial\mathbf{F}^{\mathrm{T}}}{\partial t}\,\frac{\partial\mathbf{F}}{\partial\bar{x}} + \frac{\partial\mathbf{F}^{\mathrm{T}}}{\partial\bar{x}}\,\frac{\partial\mathbf{F}}{\partial t}\right) + \left(\frac{\partial L_{Ci}}{\partial t}\right)^2\frac{\partial\mathbf{F}^{\mathrm{T}}}{\partial\bar{x}}\,\frac{\partial\mathbf{F}}{\partial\bar{x}}\right]\mathrm{d}\bar{x},$$

$$\mathbf{m}_{e2} = \int_0^{l_e(t)} J_{11}^{\rho}(L_{Ci}-\bar{x})\frac{\partial V}{\partial t}\frac{\partial\mathbf{F}^{\mathrm{T}}}{\partial\bar{x}}\,\frac{\partial\mathbf{F}}{\partial\bar{x}}\,\mathrm{d}\bar{x}. \tag{29}$$

It is clear that $\mathbf{k}_{e0}$ is the common structural stiffness matrix, but the other three matrices of $\mathbf{k}_{eq}$ are mass-dependent

components of the equivalent stiffness of the sliding beam. The damping matrix is in general non-symmetric. If the motion is such that the mass enters into the system (i.e., extrusion), then matrix $\mathbf{c}_{eq}$ is positive definite, but if the mass is leaving the system (i.e., retraction), the matrix $\mathbf{c}_{eq}$ is negative definite. After the assembling process, one can get the following expression:

$$\mathbf{M}\frac{\partial^2\mathbf{Q}}{\partial t^2}+\mathbf{C}_{eq}\frac{\partial\mathbf{Q}}{\partial t}+\mathbf{K}_{eq}\mathbf{Q}=\mathbf{0}, \tag{30}$$

where $\mathbf{M}$, $\mathbf{C}_{eq}$ and $\mathbf{K}_{eq}$ are the global matrices of mass, equivalent damping and equivalent stiffness, whereas $\mathbf{Q}$ is the global vector of nodal variables.

The damping matrix $\mathbf{C}_{eq}$ can be modified in order to account for structural damping as

$$\mathbf{C}_{eq}=\mathbf{C}_1-\mathbf{C}_2+\frac{\partial\mathbf{M}}{\partial t}+\mathbf{C}_{RD}. \tag{31}$$

The matrix $\mathbf{C}_{RD}$ corresponds to the system proportional Rayleigh damping given by

$$\mathbf{C}_{RD}=\alpha\mathbf{M}+\beta\mathbf{K} \tag{32}$$

in which $\mathbf{M}$ and $\mathbf{K}$ are the global mass and structural stiffness matrices, respectively; whereas parameters α and β are computed from two experimental modal damping functions [15,16].

The Matlab solvers are employed to simulate numerically the finite element model, for this reason Eq. (30) is represented in the following ODE form:

$$\mathbf{A}\frac{\mathrm{d}\mathbf{W}}{\mathrm{d}t}+\mathbf{B}\mathbf{W}=\mathbf{0} \tag{33}$$

in which

$$\mathbf{A}=\begin{bmatrix}\mathbf{C}_{eq} & \mathbf{M}\\ \mathbf{M} & \mathbf{0}\end{bmatrix},\quad \mathbf{B}=\begin{bmatrix}\mathbf{K}_{eq} & \mathbf{0}\\ \mathbf{0} & -\mathbf{M}\end{bmatrix},\quad \mathbf{W}=\left\{\mathbf{Q},\frac{\mathrm{d}\mathbf{Q}}{\mathrm{d}t}\right\}^{\mathrm{T}}. \tag{34}$$

3. Numerical studies

3.1. Convergence and comparisons with other approaches

In the following paragraphs convergence check and comparison among different approaches are performed. In these calculations the structural damping is neglected.

Fig. 2 shows the tip displacements for four different discretization (with two, four, six and eight elements) of a isotropic beam tested by Al-Bedoor and Khulief [7] whose properties are shown in Table 1. The deployment of the beam follows a profile for $L(t)$ given by

$$L(t)=L_0+Vt, \tag{35}$$

where $L_0=1.8\,\mathrm{m}$ is the initial length of the beam outside the hub, $V=0.3\,\mathrm{m/s}$ is the deployment velocity. For the simulation process, a tip displacement of $-0.005\,\mathrm{m}$ and null velocities are imposed in the initial state vector.

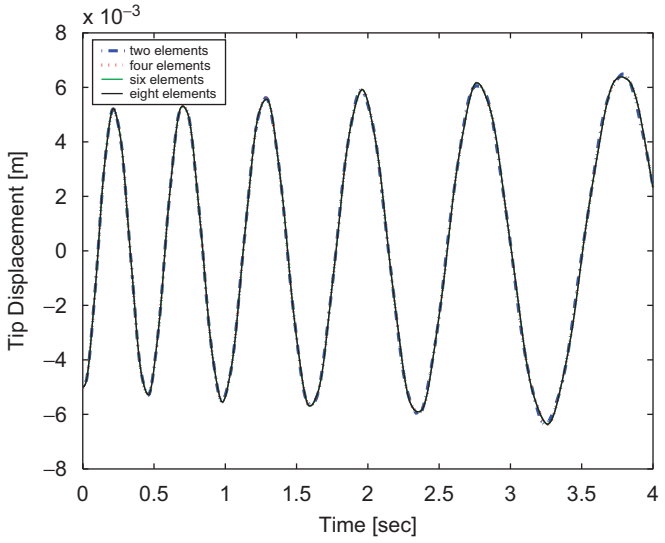

Fig. 2. Response for different discretization cases.

Table 1
Data for the aluminium beam analyzed by Al-Bedoor and Khulief [7]

Properties	Values
Total length L_T (m)	3.6
Flexural stiffness J_{11}^{11} (N/m^2)	756.65
Mass per unit length J_{11}^{ρ} (kg/m)	4.015

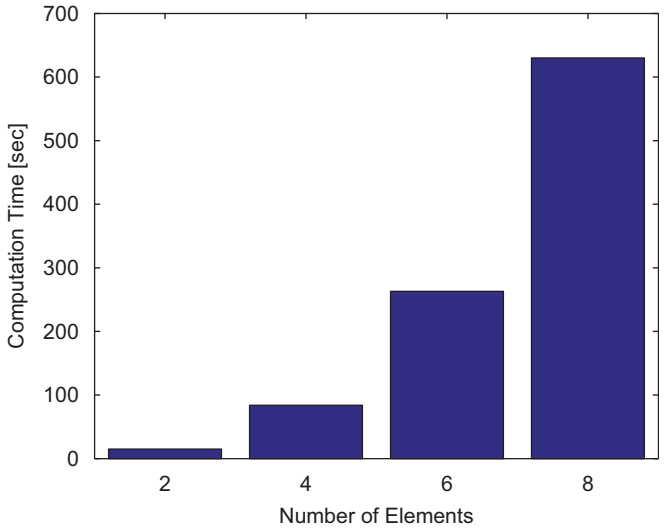

Fig. 3. Computation time for different discretization cases.

Fig. 3 shows the time consumed in the calculation (in a Pentium IV computer with 3.8 GHz, 512 RAM) of the four models. As it can be seen from Figs. 2 and 3, models with few elements can reach acceptable results in a reasonable short time.

Fig. 4 shows the tip displacement of the previous isotropic beam, comparing the present approach with the results of Al-Bedoor and Khulief [7]. Both approaches

employed beam models with four finite element, however, the last authors used a transition element formulation.

The tip displacements of the retracting beam are compared with those given by Al-Bedoor and Khulief [7] in Fig. 5. In this case the retracting pattern with the same form of expression (35), but with $L_0 = 3.0\,\mathrm{m}$, $V = -0.3\,\mathrm{m/s}$ and an initial tip displacement of $-10\,\mathrm{mm}$. For this last calculation, a model with four elements was employed. An excellent agreement between the two approaches is observed.

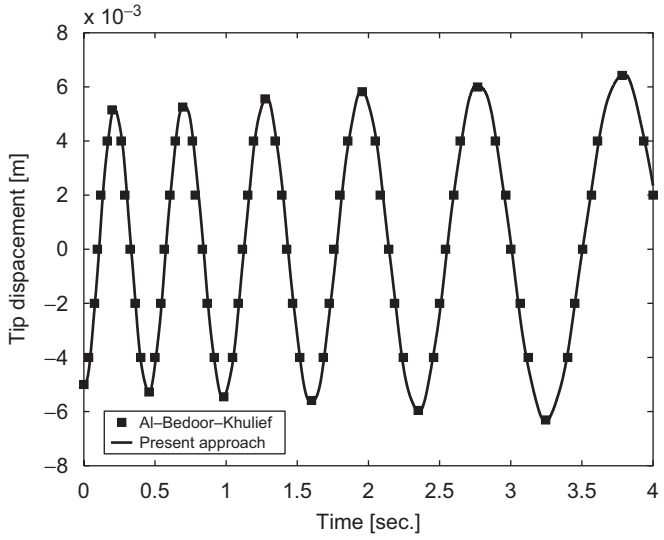

Fig. 4. Tip displacement of a deploying beam at $V = 0.3\,\mathrm{m/s}$.

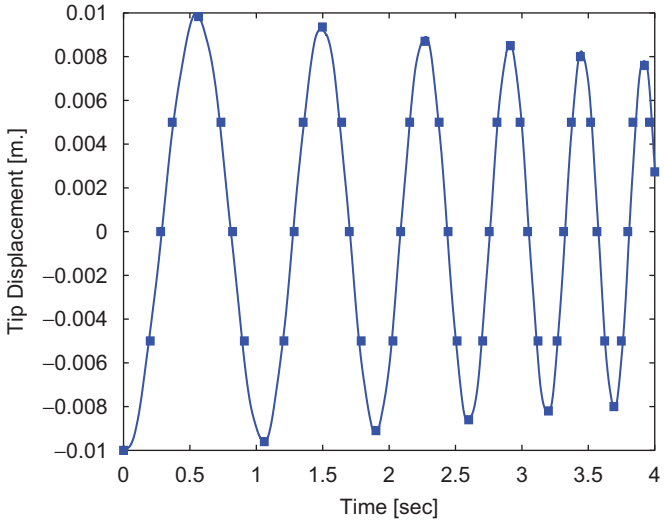

Fig. 5. Tip displacement of a deploying beam at $V = -0.3\,\mathrm{m/s}$.

3.2. Simulation of the dynamics of beams made of functionally graded materials

In this paragraph an analysis of the dynamics of sliding beams with different configurations of functionally graded properties is performed. The beam for the studies performed in this paragraph is constructed by a material whose properties vary functionally from a stainless steel surface of SUS304 to a ceramic surface of Silicon Nitride. The basic properties of these components [8,9] are given in Table 2. For all simulations the beam has a total length $L_T = 3.6\,\mathrm{m}$ and the cross-section has a mean radius $R_m = 0.025\,\mathrm{m}$ and a wall thickness $e = 0.004\,\mathrm{m}$.

As a first simulation, the two deployment profiles of expressions (36) and (37) are selected. In (36) and (37) L_0 is the initial free length of the beam, V is the sliding velocity, a is the acceleration, τ and η are constants. The deployment pattern (36) produces the deployment of the beam with a constant acceleration and contains (35) as a particular case. The pattern (37) performs the deployment of the beam with time varying velocity and acceleration. Thus, under this pattern, the beam domain evolves with pulsatile velocity (between zero and η/τ) and sinusoidal acceleration.

$$L(t) = L_0 + Vt + \frac{at^2}{2}, \tag{36}$$

$$L(t) = L_0 + \frac{\eta}{\tau}\left[t - \frac{\tau}{2\pi}\mathrm{Sin}\left[\frac{2\pi}{\tau}t\right]\right]. \tag{37}$$

Figs. 6and 7 show the tip displacement of a beam under the extrusion corresponding to deployment laws (36) and (37), respectively. For both simulation models with four elements and imposing an initial tip displacement of $-5\,\mathrm{mm}$ were employed and a functionally graded material with a ceramic outer surface and a metallic inner surface was adopted. No structural damping and temperature effects were considered. The properties for the deployment

Table 2
Properties of stainless steel (SUS304) and silicon nitride (Si_3N_4)

Properties	Material	m_{p0}	c_0	c_1	c_2	c_3
E (N/m^2)	SUS304	2.0104×10^{11}	0	3.0790×10^{-4}	-6.534×10^{-7}	0
	Si_3N_4	3.4843×10^{11}	0	-3.0700×10^{-4}	2.160×10^{-7}	-8.946×10^{-11}
v	SUS304	0.3262	0	-2.0020×10^{-4}	3.797×10^{-7}	0
	Si_3N_4	0.2400	0	0	0	0
ρ (kg/m^3)	SUS304	8166	0	0	0	0
	Si_3N_4	2370	0	0	0	0

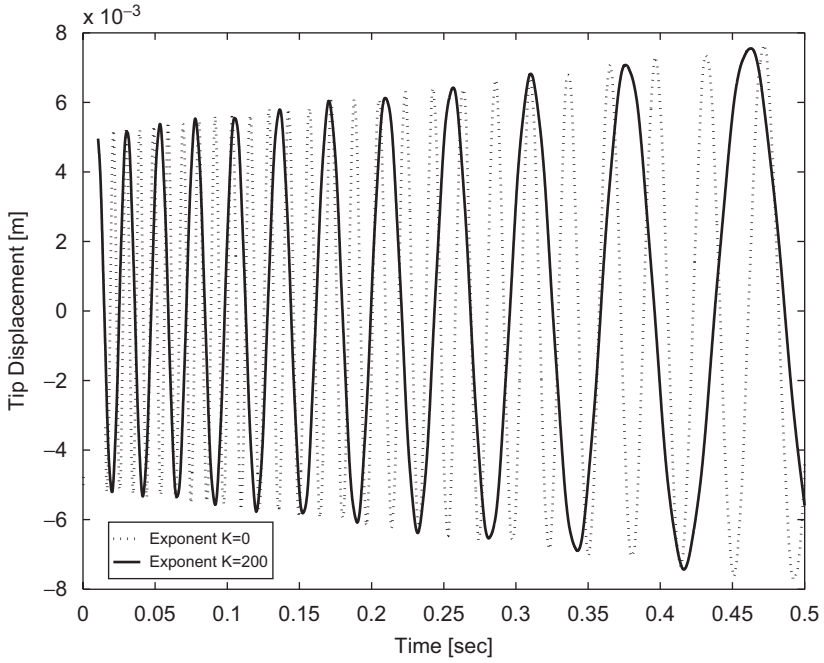

Fig. 6. Tip displacement of a deploying beam with a constant acceleration pattern.

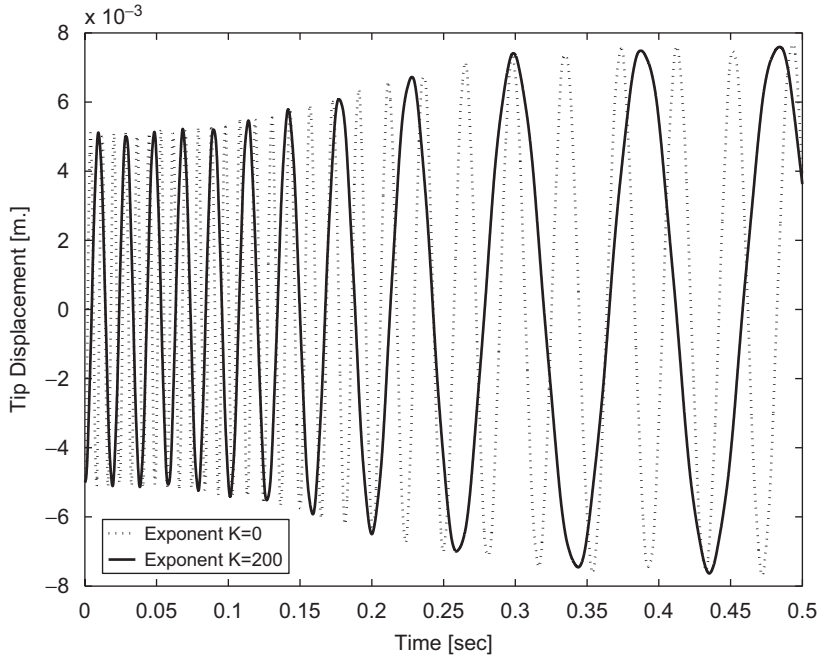

Fig. 7. Tip displacement of a deploying beam with a sinusoidal acceleration pattern.

law (36) were $L_0 = 1\,\mathrm{m}$, $V = 2\,\mathrm{m/s}$ and $a = 3\,\mathrm{m/s^2}$; whereas for deployment law (37), $L_0 = 1\,\mathrm{m}$, $\eta = 0.7$ and $\tau = 0.2$. In both figures it is possible to see the high frequency oscillating deployment when the exponent $K = 0$ because the beam is totally made of ceramic which has a high stiffness.

It is easy to modify the finite element formulation in order to account for a lumped tip mass M_T (see Ref. [1]). Just a lumped mass term has to be added in the tip node and the factor $J^{\rho}_{11}(L_{Ci} - \bar{x})$ in the matrix $\mathbf{m}_{e2}$ has to be changed by $(J^{\rho}_{11}(L_{Ci} - \bar{x}) + M_T)$.

Fig. 8 shows the time history of the tip displacement of a beam with an exponent of $K = 200$ deploying with the law (37), where $L_0 = 1\,\mathrm{m}$, $\eta = 0.8$ and $\tau = 0.2$. In this study, the structural damping and the thermal effects are not considered. In one case a tip mass of $M_T = 1\,\mathrm{kg}$ (which

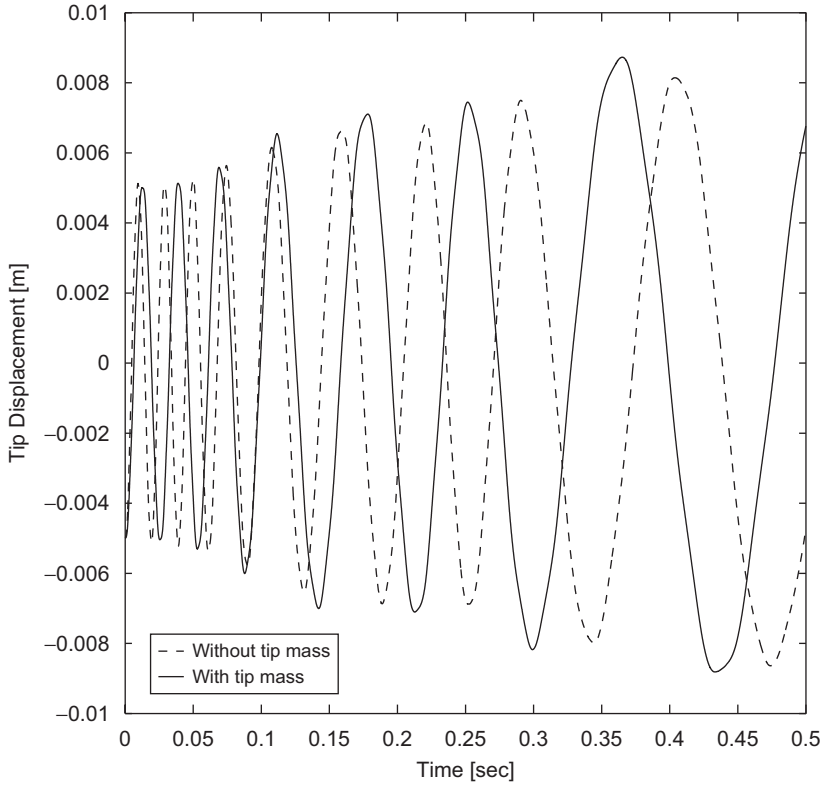

Fig. 8. Effect of the tip mass on the tip displacement for a sinusoidal acceleration pattern, $K = 200$.

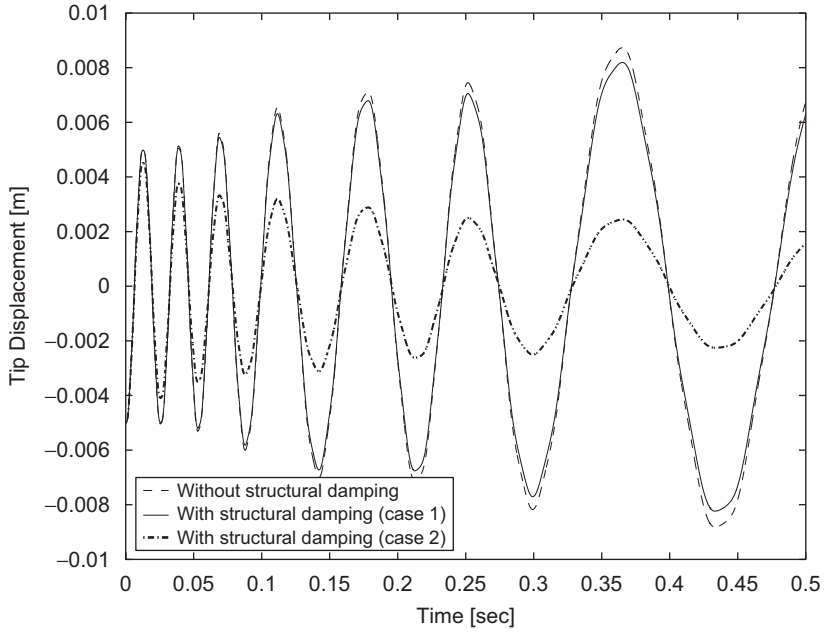

Fig. 9. Tip displacement. Analysis of structural damping, $K = 200$.

is approximately the 20% of the initial mass of the protruded bar, i.e., at $t = 0$) is considered. As it was expected, the addition of a tip mass has the effect of lowering the frequency of oscillations during the extrusion.

A final analysis evaluates the effect of structural damping with the inclusion of tip mass. The coefficients α and β are calculated [15] assuming for simulation purposes the damping coefficients ξ_1 and ξ_2 for the first and second frequencies, respectively. Two cases are simulated. In "case 1", the damping coefficients are $\xi_1 = 1 \times 10^{-6}$ and $\xi_2 = 5 \times 10^{-6}$, and in "case 2" the damping coefficients are $\xi_1 = 2 \times 10^{-5}$ and $\xi_2 = 1 \times 10^{-4}$. Fig. 9 compares the time histories of the tip displacement for a beam with $K = 200$ and a tip mass of $M_T = 1\,\text{kg}$, taking into account and

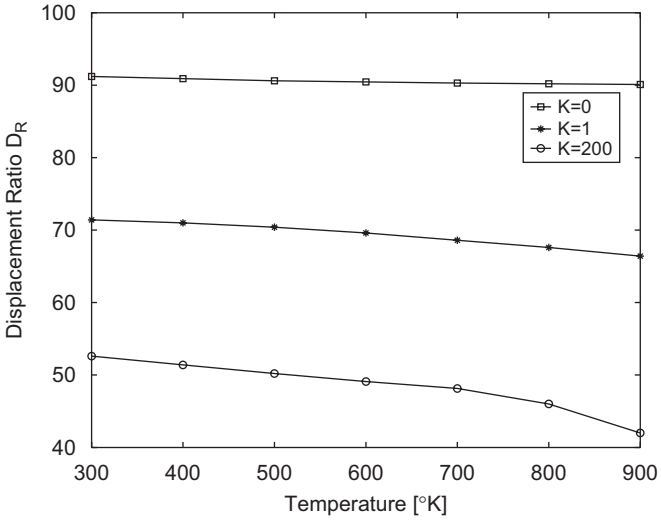

Fig. 10. Variation of displacement ratios D_R with the temperature.

neglecting the structural damping. The deployment characteristics are the same to those of the cases of Fig. 8. As it can be seen, in "case 1" the motion is lightly damped, on the contrary "case 2" shows a more pronounced damping in the tip displacement of the system since the damping coefficients employed in the calculation of Rayleigh damping are twenty times greater than the ones employed in "case 1". Fig. 10 compares the variation of the displacement ratio D_R (38) of the tip displacement (i.e., relative to the initial condition) with respect to the temperature for different configurations of FGM.

$$D_R = \max\left|\left(1 - \frac{v(L, t>0.5)}{v(L,0)}\right)100\right|. \tag{38}$$

The data plotted in Fig. 10 correspond to a beam deploying according to (37) with $L_0 = 1\,\mathrm{m}$, $\eta = 0.8$ and $\tau = 0.2$, $M_T = 1\,\mathrm{kg}$ and the damping coefficients of "case 2", that is $\xi_1 = 2 \times 10^{-5}$ and $\xi_2 = 1 \times 10^{-4}$. Note that as the beam is mainly composed by ceramics ($K \to 0$) the effect of proportional structural damping is not very significant and practically it is not affected by the increase of temperature. Conversely, if the beam has an sensible proportion of the metallic component ($K \to \infty$) the damping effects are quite significant and affected by the increase of temperature.

4. Conclusions

In this article a formulation for axially moving beams made of functionally graded materials was developed. The structural model is based on the Bernoulli–Euler hypotheses including the constitutive equations for a ceramic-metallic functionally graded material. The variation of properties along the wall thickness of the annular cross-section follows a simple exponential law.

A finite element formulation was employed to simulate the dynamics of extruding and retracting beams. This formulation considers the use of a beam element of variable length which showed a very good performance.

The finite element results obtained with this formulation for the tip displacement of a sliding beam, agrees well with the results published by other authors employing the assumed modes methods.

Two different patterns, or laws of deployment, were tested in the protrusion of functionally graded beams. The variation of the properties, by means of the exponent K, was analyzed. The simulation results showed that a beam in which the ceramic is the main component has a high oscillatory deployment but when the beam has a metallic main component the frequency of oscillation is lower. Moreover, as the beam is mainly composed by a metallic part, the damping is quite sensible and it is strongly affected by the temperature. However, if the beam is mainly composed by ceramic substrates, the structural damping has scarce influence

As a final conclusion, this kind of model is quite useful for the analysis of deploying beam-like structures with specified deploying patterns, for both functionally graded and isotropic materials. Although the model presents a relative complexity in its formulation (due to the concept of element with variable length), it has a good computational performance.

Acknowledgments

This work was partially supported by CNPq, Project 302135/84-7, and by Faperj through a Bolsa Cientistas do Nosso Estado. Grant 152117/2004-0 of CNPq, the support of Universidad Tecnológica Nacional, Facultad Regional Bahía Blanca and CONICET are also acknowledged.

References

[1] Stylianou M, Tabarrok B. Finite element analysis of an axially moving beam, Part I: time integration. Part II: stability analysis. J Sound Vib 1994;178(4):433–73.
[2] Behdinan K, Stylianou M, Tabarrok B. Dynamics of flexible sliding beams non-linear analysis. Part I: formulation. J Sound Vib 1997;208(4):517–39.
[3] Behdinan K, Stylianou M, Tabarrok B. Dynamics of flexible sliding beams—non-linear analysis, Part II: transient response. J Sound Vib 1997;208(4):541–65.
[4] Theodore RJ, Arakeri JH, Ghosal A. The modelling of axially translating flexible beams. J Sound Vib 1996;191(3):363–76.
[5] Imanishi E, Sugano N. Vibration control of cantilever beams moving along the axial direction. JSME Int J Ser C 2003;46(2):527–32.
[6] Al-Bedoor BO, Khulief KA. Vibrational motion of an elastic beam with prismatic and revolute joints. J Sound Vib 1996;190(2):195–206.
[7] Al-Bedoor BO, Khulief YA. General planar dynamics of a sliding flexible link. J Sound Vib 1997;207(5):641–61.
[8] Reddy JN, Chin CD. Thermomechanical analysis of functionally graded cylinders and plates. J Therm Stresses 1998;21:593–626.
[9] Oh SY, Librescu L, Song O. Thermoelastic modeling and vibrations of functionally graded thin-walled rotating blades. AIAA J 2003;41(10):2051–60.

[10] Tanigawa Y. Some basic thermoelastic problems for nonhomogeneous structural materials. Appl Mech Rev 1995;48:287–300.
[11] Kadoli R. Ganesan N. Buckling and free vibration analysis of functionally graded cylindrical shells subjected to a temperature-specified boundary condition. J Sound Vib 2006;289:450–80.
[12] Praveen GN, Chin CD, Reddy JN. Thermoelastic analysis of functionally graded ceramic-metal cylinder. J Eng Mech 1999;125: 1259–67.
[13] Cortinez VH, Piovan MT. Vibration and buckling of composite thin walled beams with shear deformability. J Sound Vib 2002;258(4):701–23.
[14] McIver DB. Hamilton's principle for a system of changing mass. J Eng Math 1973;7:249–61.
[15] Bathe KJ. Finite element procedures in engineering analysis. Englewood Cliffs, New Jersey: Prentice-Hall; 1982.
[16] Meirovitch L. Principles and techniques of vibrations. Upper Saddle River, New Jersey: Prentice-Hall; 1997.